On avalanche measurements at the Norwegian full-scale test-site Ryggfonn

Peter Gauer[1,2*], Karstein Lied[1], and Krister Kristensen[1]

[1] Norwegian Geotechnical Institute
Sognsveien 72, NO-0806 Oslo, Norway
[2] International Centre for Geohazards, c/o NGI

ABSTRACT. Avalanche measurements and observations that were carried out at the Ryggfonn test site, Norway, on 16 April 2005 are analyzed. The data include pulsed Doppler radar measurements, impact pressure readings from load cells mounted at two locations within the track and stress readings from load plates flush with the upstream slope of a catching dam. The radar measurements were used to derive velocities and estimates on the retarding acceleration. The retarding accelerations show a wide discrepancy with commonly used model assumptions. Pressure measurements were combined with velocity measurements. The measurements infer that commonly used drag factors are not sufficient to describe force exert by slow moving wet snow. Measurements with load plates imply plastic failure rather then Coulomb-type friction. Field observation of the avalanche track suggest that erosion / abrasion due to (saltating) particles is one possible entrainment mechanism.

Keywords: avalanche, full-scale measurements, velocity, acceleration, impact pressure, shear stress

1 INTRODUCTION

There are only a few dedicated full-scale avalanche test-sites; full-scale avalanche in the sense that avalanche of size 4 and more could be observed. Probably, one of the first sites was the Russian site at Khibini, cf. (Kotlyakov et al., 1977; Bozhinskiy and Losev, 1998). Certainly, also the measurements at Rogers pass belong in the line of early full-scale measurements (McClung and Schaerer, 1985; Schaerer and Salway, 1980). The Ryggfonn site is operated by the Norwegian Geotechnical Institute since 1980. Early measurements from this site can be found in (Norem et al., 1985; Bakkehøi et al., 1981). In Japan, the Kurobe Canyon serves as instrumented full-scale test-site Kawada et al. (1989); Nishimura et al. (1989, 1993). Since 1997/1998, the Swiss test side Vallée de la Sionne / Valias is in full operation (Ammann, 1999). However, also its predecessor should be mentioned; although, mostly only radar measurements were done at Lukmanier Pass, Val Medel / Grisons (Gubler, 1987; Salm and Gubler, 1985). A comprehensive overview of the European sites can be found in (Issler, 1999), and an updated version of this in (Barbolini and Issler, 2006).

Although measurements of full-scale avalanches are expensive and time consuming, and they are a difficult to perform under those harsh conditions within an avalanche (and not always easy to understand), they are indispensable to gain in-depth understanding of the flow behavior of avalanches. They are needed to crosscheck the scaling used in small-scale experiments. They also form the basis for developing and calibrating models. Information on experimental techniques and sensors can be found in (Issler, 2003).

In the following we focus on measurements and observations from one full-scale event (20060416 15:00) at Ryggfonn.

2 RYGGFONN TEST-SITE

The Norwegian Geotechnical Institute (NGI) operates the full-scale avalanche test-site Ryggfonn, Western Norway, over more than 25 years. The test-site is characterized by a north facing bowl in the upper part of the track, a vertical drop of about 900 m in total, and a horizontal track length of about 2000 to 2100 m at max. The mean inclination of the main track is about 29°. Typical avalanche sizes range between 2 (mass of 100 Mg) and 4 (mass of 10 000 Mg), may reach even class 5, according to the Canadian snow avalanche size classification and maximum front velocities are up to 60 m s^{-1}. Observations include dry and wet snow avalanches. Figure 1 gives an overview of the test site.

During the years, the instrumentation has changed. At present, measurements from Ryggfonn avalanche test-site include pressure readings from five load cells with a size of 1.2 $\times$ 0.6 m^2 at two locations in the lower third of the track. At a 16 m high catching dam in the runout zone, normal and shear stresses are measured on two places. The crown width of the dam is 75 m. In addition, six geophones are placed in the ground in the run-out zone. Recently,

*Corresponding author's address:
Peter Gauer
Norwegian Geotechnical Institute,
P.O. Box 3930 Ullevål Stadion, NO–0806 Oslo, Norway
Tel: ++47 22 02 31 29; Fax: ++47 22 23 04 48; E-mail: pg@ngi.no

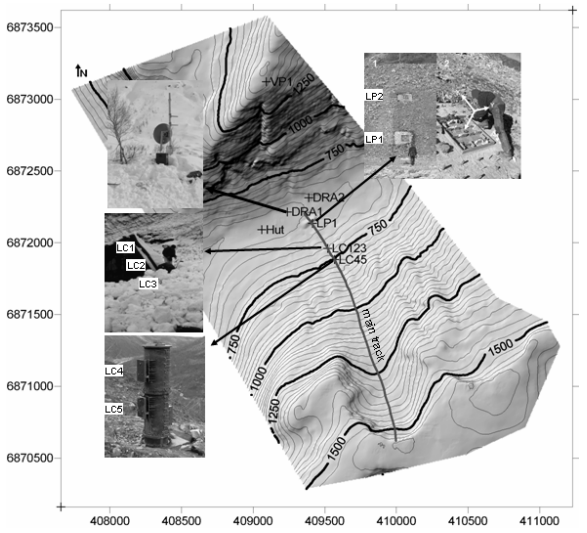

Figure 1: Overview of the Ryggfonn test site (UTM). The view shows the line of the main track, the locations of the load cells (LC45 and LC123) and the placement of the load plates in the dam (LP1 and LP2). In addition, two Doppler radar positions are indicated (DRA1 and DRA2).

two pairs of FMCW Doppler radar were also buried in the lower part of the track. These should provide flow height information, information on erosion, and, hopefully, on the vertical velocity profile. Additionally, NGI owns a pulsed Doppler radar for velocity measurements along the track.

3 MEASUREMENTS AND OBSERVATIONS

Table 1: Avalanche characterization. The avalanche is also documented in (Gauer and Kristensen, 2005).

Date yyyymmdd hh:mm	Size	Classification (ICSI) A	B	C	D	E	F	G	H	J
20050416 15:00	4	4	7	1	2	7/2	3	7	3	4

On 16 April 2006 a size 4 avalanche was released by detonating 150 kg of explosives buried in the top cornice at ridge line above the bowl. Preceding the event were nearly two months of stable weather and snow conditions. The first part of April showed a period of snowfall and southwest winds favoring blowing and drifting snow. Around the 15th, the weather cleared and the same day a small avalanche ran in the lower path as a result of afternoon sunshine.

The weather during the release was sunny and calm with 0.25 m fresh snow deposition from the previous days. At 1420 m a.s.l. the air temperature was -2.5 °C with high temperatures of -1.5 °C the preceding 24 hours. Southwesterly winds blow at 2 m s^{-1} with gusts up to 5 m s^{-1}. In the runout zone the air temperature was about 5 °C at the time of release.

The avalanche started out as dry-mixed one. At the end of the bowl it nearly came to halt, but it picked up some speed again in the steeper lower section of the track.

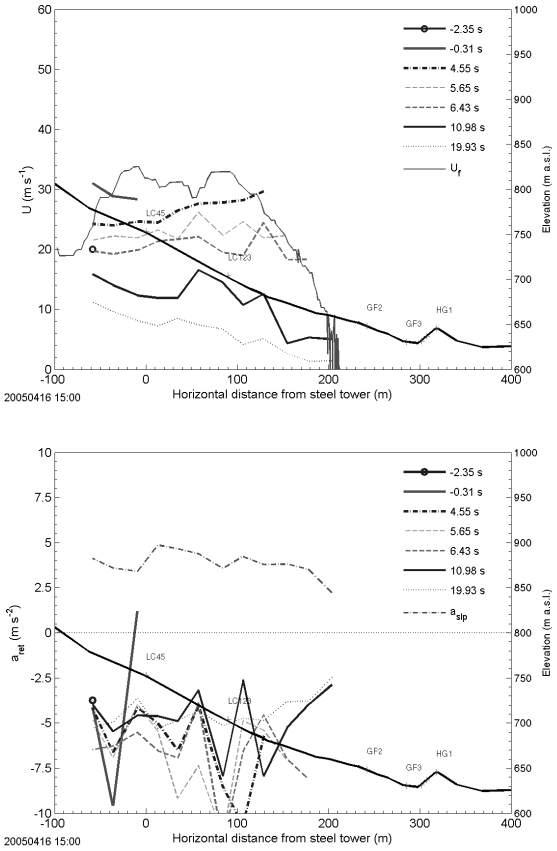

Figure 2: Avalanche 20050416 15:00: Velocity and acceleration vs. location along the lower track for seven instants in time. The upper panel shows the averaged velocity and the lower panel the retarding acceleration derived from the respective pair of adjoining range gates of the Doppler radar. In addition, the thin solid line in the upper panel shows the front velocity. The dashed dotted line in the lower panel gives $a_{slp} = g \sin \phi$. The thick solid line gives the path profile in the lower part of the track.

There it eroded a substantial amount of snow and probably triggered a second wet slide. Table 1 gives a characterization of the event following the Canadian size classification (cf. McClung and Schaerer, 1993) and the International Avalanche Classification (Avalanche Atlas, UNESCO, 1981).

3.1 Velocity measurements

During this event, it was possible to gain pulsed Doppler radar measurements from the lower part of the track (below about 800 m a.s.l.). Figure 2 depicts velocity measurements and derived retarding accelerations for seven instants in time (measured relative to the arrival time at the steel tower). In addition, the front velocity is shown in the upper panel and in the lower panel the driving (slope parallel) component of the gravity, $a_{slp} = g \sin \phi$, is given. The retarding acceleration, a_{ret}, is calculated by

$$a_{ret} = a - g \sin \phi \,, \qquad (1)$$

where g is the gravitational acceleration and ϕ the slope angle (positive down slope). a is the effective acceleration of a part of the avalanche ("fictitious mass block") within the avalanche. (This is the one that is derived from the velocity measurements). For an explanation on the derivation of a, we refer to Gauer et al. (in press,s). The retarding acceleration is a measure for the resisting forces acting on the avalanche.

At the time as the avalanche enters the area covered by the radar, it is accelerating and the velocity of the frontal part increases. Usually, the head velocity tends to be higher then that of the body and tail until the avalanche starts to stop. This can also be seen from the velocity profiles shown in Figure 4. At the height of the concrete wedge the avalanche starts to decelerate rapidly. Retarding accelerations are as high as $\approx 12\,\mathrm{m\,s^{-2}}$ (absolute value). The dry part at the front stopped about 75–100 m short of the dam. The wet part continued to flow slowly another approximately 2 minutes piling up in front of the dam.

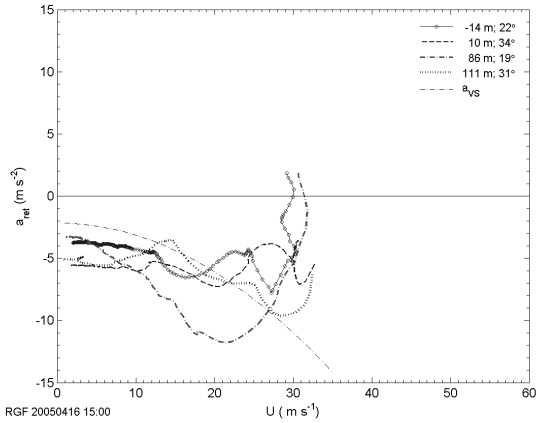

Figure 3: Avalanche 20050416 15:00: Retarding acceleration vs. velocity at for points. The first two correspond points just above and below the steel tower (LC45) and the other two to points above and below the concrete wedge (LC123). Numbers give the relative position to the steel tower and the mean slope angle at those points. a_{VS} is the retarding component according to (2).

Figure 3 plots the retarding acceleration vs. velocity for four location as the avalanche passes by. This is a kind of Eulerian representation; a Lagrangian representation can be found in (Gauer et al., submitted). No unambiguous relation between retarding acceleration and velocity evident. The mean slope angle at the steel tower is approximately 30° and at the concrete wedge about 26°. At low velocities ($\lesssim 10\,\mathrm{m\,s^{-1}}$) three of the four plots imply velocity independency. In addition to the derived retarding acceleration, the resistance component as it would be given, e.g., in a Voellmy-Salm type model is shown:

$$a_{VS} = -g\left(\mu\,\cos\phi + \frac{u^2}{\xi\,h_a}\right)\,. \qquad (2)$$

The parameter used are estimates, but they are in accordance to the Swiss guide lines; $\mu = 0.25$, $\xi = 1000\,\mathrm{m\,s^{-2}}$, and $h_a = 1.5\,\mathrm{m}$. The slope angle for this example is 28°.

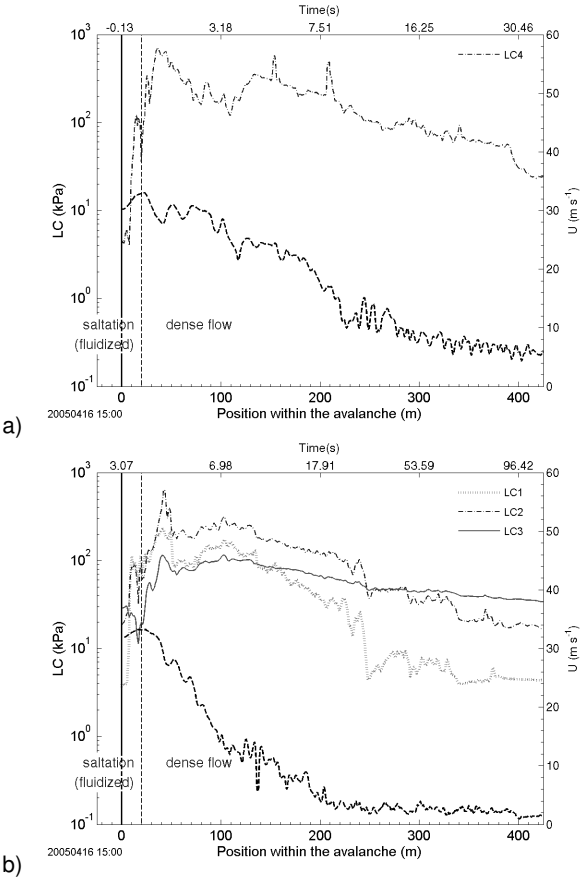

Figure 4: Avalanche 20050416 15:00: Load cell measurements: pressure vs. position within the avalanche; a) at steel tower and b) at the concrete wedge. Note the logarithmic scaling of the left ordinate and the different horizontal scaling. Values are running means with 25 m filter width. The black dashed lines show the corresponding velocity profiles. (LC5, which is not shown, was totally buried and LC3 was initially partial buried at that time.)

Obviously, the model would underestimate the resistance at low velocities whereas it overestimates it at high speeds.

3.2 Pressure measurements

Figure 4 shows the measured impact pressure and the corresponding velocity distribution. Here, the position within the avalanche is a measure of distance behind the front as it passes the sensor. (It is similar to the wind run.) The measured pressures of up to 600 to 800 kPa are surprisingly high. These pressures are probably related to the damp or wet snow slide behaving like a cohesive flow a high shear strength, but could also be attributed to some large and hard snow blocks originating from the cornice, or combination of both. At the front of the avalanche we still observe a fluidized (saltation) layer before the more dense part arrives. If one relates the measured pressure values, LC, to the dynamic pressure one can attain an estimate of the combination of density and drag factor

$$\rho\,C_D = \frac{2\,LC}{A_e\,U^2}\,, \qquad (3)$$

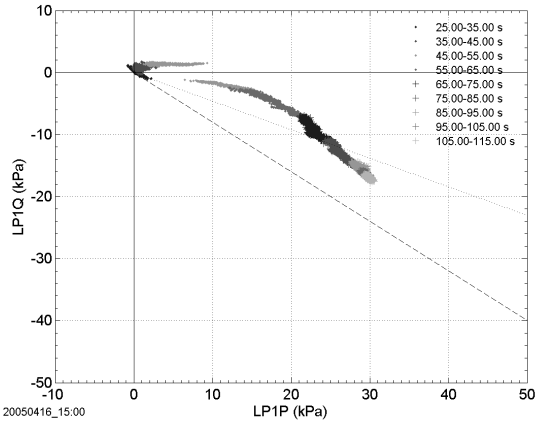

Figure 5: Avalanche 20050416 15:00: Load plate measurements: Shear stress vs. normal stress at the sliding plane (surface of the snowpack) along the dam slope. Shown is the lower plate LP1. Q is the total traction and P the normal stress at the sliding plane. The dashed line in the panel corresponds to the ratio between shear and normal stress in the case of static loading ($-\tan 40^\circ$ or $-\tan 20^\circ$).

where A_e is the effected sensor area and U the measured velocity. If one further assumes a density, ρ, between 300 and 500 kg m^{-3} within the slowly moving tail, one finds a C_D of approximately 20 to 40 for LC2 there. Values that are typically proposed for C_D are in the order of $\mathcal{O}$(2-6), cf. (Norem, 1990; Salm et al., 1990; Mellor, 1968). The measurements indicate that the drag factor depends much more on the flow regime as commonly recognized. Especially, the force in slow moving avalanche might be considerably underestimated.

3.3 Load plate measurements

Figure 5 shows the total traction Q versus the normal pressure, P, at the sliding surface (boundary between snowpack and avalanche). For a detailed explanation how the measurements at the load plates can be related to the sliding surface, we refer to Gauer et al. (in press). Only the slow moving wet part arrived at the dam and slowly loaded the load plate. On arrival of the avalanche, the shear stress increases with the normal stress (t = 35 – 45 s). Then, a shear (plastic) failure is obvious (t = 45 – 55 s), i.e., the shear stress is independent of the normal stress. In this case, the yield stress is about 1.5 – 2 kPa. Thereafter, the plot shows basically a static loading. In this case one would expect $Q/P = -\tan\phi_e$, where ϕ_e is the effective slope angle. The dam slope is about 40°, the slope of the deposit in front of the dam prior to the event was about 20°. To give an impression of the final stage, Figure 6 depicts a snapshot of the deposit. The height over the load plate is about 8 m of fresh deposit.

Figure 6: Avalanche 20050416 15:00: Snapshot from the deposits. The arrow indicate the approximate location of the load plate, however the main deposit is slightly of. (Photos by Arne Moe/NGI.)

4 Erosion

One of the puzzling questions, which was disregarded for awhile after first descriptions by, e.g. (Grigorian and Ostroumov, 1977; Eglit, 1983; Brugnot and Pochat, 1981; Mellor, 1968; Hopfinger and Tochon-Danguy, 1977), but caught recently new attention (Sovilla et al., 2001; Sovilla, 2004), is the question of mass balance and erosion mechanism. Gauer and Issler (2004) proposed several possibilities, among others erosion / abrasion due to (saltating) particles. Figure 7 shows snapshots from the track during and after the avalanche descent at about the same location. The erosion of the snowpack by the avalanche is obvious. The scratch marks remind one at abrasion due to particles or clods.

5 DISCUSSION AND CONCLUSIONS

Measurements and field observations of an artificially released avalanche at the full-scale avalanche test-site Ryggfonn, Norway are presented.

Velocity measurements using Pulsed Doppler radar and derived retarding acceleration infer that friction terms in several classic avalanche models (for example Salm et al. (1990); Perla et al. (1980)) are overestimating the resistance at high avalanche speeds and underestimated it in the runout phase. This has consequences in respect to hazard zoning.

Pressure measurements with large size load plate suggest that the drag factor in the slow-moving wet part of the avalanche can reach values of 20 to 40, which is far more than commonly used. With even such basic things as the drag coefficient not yet understood there is clearly much more research that should be undertaken in this area.

Field observations of scratch marks in the remaining snowpack along parts of the track and video analysis from the avalanche event indicate that substantial entrainment occurred and that erosion / abrasion due to saltating particles is a possible mechanism (cf. Gauer and Issler, 2004). However, there is definitely more work to be done to ob-

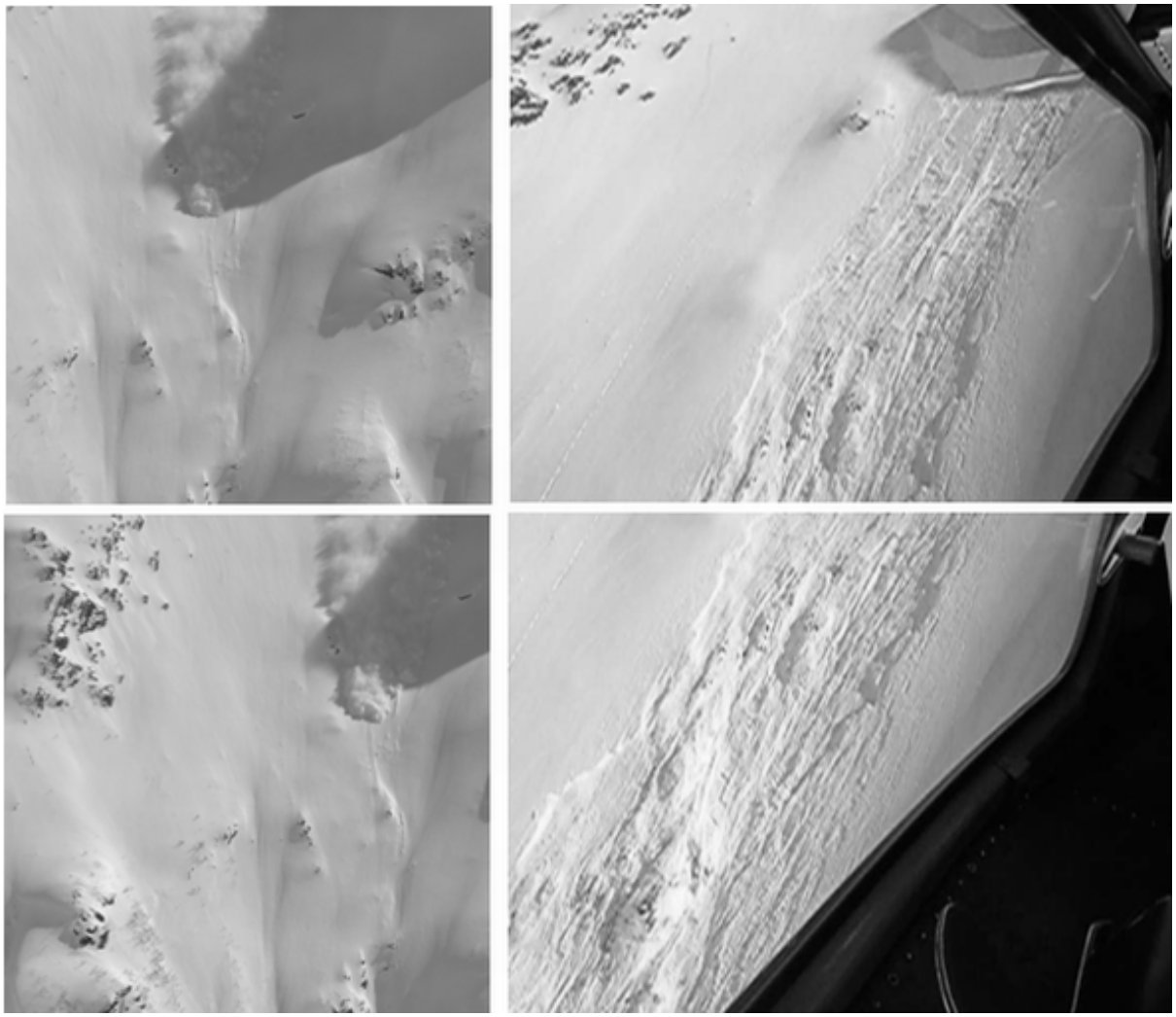

Figure 7: Avalanche 20050416 15:00: Snapshots from the track. Left hand side: during the descent of the avalanche; right hand side after the event (similar location). Obviously, the avalanche eroded during the descent. Scratch marks remind one at erosion / abrasion due to (saltating) particles. (Photos by Arne Moe/NGI)

tain a better understanding of the mass balance and the involved mechanisms.

Still further work is needed to combine results from different sensors to construct an even clearer picture of the avalanche structure. At the Ryggfonn site, we hope, for example, to gain further insight from the FMCW-radars in the next years. However, as some of the observations might be specific to the avalanche path, it is important to cross-check results from Ryggfonn with measurements from other test sites, which needs an international cooperation.

ACKNOWLEDGMENTS

This work was funded through NGI's SIP-program "Avalanche research" and through the EU-Program "SATSIE (Avalanche Studies and Model Validation in Europe)" within the 5th Framework Program, EU Contract no. EVG1-CT2002-00059. We are also grateful to those who helped during the field work. These were: M.-A. Baillifard, R. Fromm, E. Lied, A. S. Moe, L. Rammer and I. Vilajosana.

REFERENCES

Ammann, W. J., 1999: A new Swiss test-site for avalanche experiments in the Vallée de la Sionne/Valais. *Cold Regions Science and Technology*, **30**, 2–11.

Bakkehøi, S., U. Domaas, and K. Lied, 1981: Calculations of snow avalanche runout distance. *Annals of Glaciology*, **4**, 24–28.

Barbolini, M. and D. Issler, 2006: Avalanche Test Sites and Research Equipment in Europe: An Updated Overview. Final-Report Deliverable D8, SATSIE Avalanche Studies and Model Validation in Europe.

Bozhinskiy, A. N. and K. S. Losev, 1998: The Fundamentals of Avalanche Science. Mitt. Eidgenöss. Inst. Schnee- Lawinenforsch. 55, Mitt. Eidgenöss. Inst. Schnee- Lawinenforsch., Davos, EISLF Flüelastr 11. CH-7260 Davos.

Brugnot, G. and R. Pochat, 1981: Numerical simulation study of avalanches. *J. Glaciol.*, **27**, 77–88.

Eglit, E. M., 1983: Some mathematical models of snow avalanches. *Advances in the Mechanics and the Flow of Granular Materials*, M. Shahinpoor, ed., Trans Tech Publications, Clausthal-Zellerfeld, Germany, volume II, 1st edition, 577–588.

Gauer, P. and D. Issler, 2004: Possible erosion mechanisms in snow avalanches. *Annals of Glaciology*, **38**, 384–392.

Gauer, P., D. Issler, K. Lied, K. Kristensen, H. Iwe, E. Lied, L. Rammer, and H. Schreiber, in press: On full-scale avalanche measurements at the Ryggfonn test site, Norway. *Cold Region Science and Technology*.

Gauer, P., M. Kern, K. Kristensen, K. Lied, L. Rammer, and H. Schreiber, submitted: On pulsed doppler radar measurements of avalanches and their implication to avalanche dynamics. *Cold Region Science and Technology*.

Gauer, P. and K. Kristensen, 2005: Avalanche Studies and Model Validation in Europe, SATSIE: Ryggfonn measurements Winter 2004/2005. NGI Report 20021048-8, Norwegian Geotechnical Institute, Sognsveien 72, N-0806 Oslo.

Grigorian, S. S. and A. V. Ostroumov, 1977: Matematicheskaya model sklonovih processov lavinnogo tipa [The mathematical model for slope processes of avalanche type] (in Russian). Scientific Report 1955, Institute for Mechanics, Moscow State University, Moscow, Russia.

Gubler, H., 1987: Measurements and modelling of snow avalanche speeds. *Avalanche Formation, Movement and Effects*, B. Salm and H.-U. Gubler, eds., number 162 in IAHS Publ., 405–420.

Hopfinger, E. J. and J.-C. Tochon-Danguy, 1977: A model study of powder-snow avalanches. *Journal of Glaciology*, **19**, 343–356.

Issler, D., 1999: European Avalanche Test Sites: Overview and Analysis in View of Coordinated Experiments. Mitteilungen 59, Eidgenöss. Inst. Schnee- Lawinenforsch., Davos, Flüelastr 11. CH-7260 Davos.

— 2003: Experimental information on the dynamics of dry-snow avalanches. *Dynamic Response of Granular Materials under Large and Catastrophic Deformations*, K. Hutter and N. Kirchner, eds., Springer, volume 11 of *Lecture Notes in Applied and Computational Mechanics*, 109–160.

Kawada, K., K. Nishimura, and N. Maeno, 1989: Experimental studies on a powder-snow avalanche. *Annals of Glaciology*, **13**, 129–134.

Kotlyakov, V. M., B. N. Rzhevskiy, and V. A. Samoylov, 1977: The dynamics of avalanching in the khibins. *Journal of Glaciology*, **19**, 431–439.

McClung, D. and P. Schaerer, 1993: *The Avalanche Handbook*. The Mountaineers, (1011 SW Klickitat Way), Seattle, Washington 98134, USA.

McClung, D. M. and P. A. Schaerer, 1985: Characteristics of flowing snow and avalanche impact pressures. *Annals of Glaciology*, **6**, 9–14.

Mellor, M., 1968: Cold Regions Science and Engineering. Part III: Engineering, Section A3: Snow Technology Avalanches, Cold Regions Research & Engineering Laboratory, Hanover, New Hampshire.

Nishimura, K., N. Maeno, K. Kawada, and K. Izumi, 1993: Structures of snow cloud in dry-snow avalanches. *Annals of Glaciology*, **18**, 173–178.

Nishimura, K., H. Narita, N. Maeno, and K. Kawada, 1989: The internal structure of powder-snow avalanches. *Annals of Glaciology*, **13**, 207–210.

Norem, H., 1990: Ryggfonn-prosjektet. NGI Report 581200-16, Norwegian Geotechnical Institute, Sognsveien 72, N-0806 Oslo, (in Norwegian).

Norem, H., T. K. Kvisterøy, and B. D. Evensen, 1985: Measurements of avalanche speeds and forces: Instrumentation and preliminary results of the Ryggfonn project. *Annals of Glaciology*, **6**, 19–22.

Perla, R., T. T. Cheng, and D. M. McClung, 1980: A two-parameter model of snow-avalanche motion. *Journal of Glaciology*, **26**, 197–207.

Salm, B., A. Burkard, and H. U. Gubler, 1990: Berechnung von Fliesslawinen. Eine Anleitung für Praktiker mit Beispielen. Mitt. Eidgenöss. Inst. Schnee- Lawinenforsch. 47, 37 pages, SLF, Davos, Switzerland.

Salm, B. and H. Gubler, 1985: Measurement and analysis of the motion of dense flow avalanches. *Annals of Glaciology*, **6**, 26–34.

Schaerer, P. A. and A. A. Salway, 1980: Seismic and impact-pressure monitoring of flowing avalanches. *Journal of Glaciology*, **26**, 179–187.

Sovilla, B., 2004: *Field experiments and numerical modelling of mass entrainment and deposition processes in snow avalanches*. Ph.d thesis, ETH Zurich.

Sovilla, B., F. Sommavilla, and A. Tomaselli, 2001: Measurements of mass balance in dense snow avalanche events. *Annals of Glaciology*, **32**, 230–236.

UNESCO, 1981: *Avalanche Atlas*. International Commission on Snow and Ice of the International Association of Hydrological Sciences, IAHS.